MEMS ENABLES OSCILLATORS WITH
SUB-PPM FREQUENCY STABILITY AND SUB-PS JITTER

R. Melamud, P.M. Hagelin, C.M. Arft, C. Grosjean, N. Arumugam,
P. Gupta, G. Hill, M. Lutz, A. Partridge, F. Assaderaghi
SiTime Corporation, Sunnyvale, California, USA

ABSTRACT

An integrated MEMS thermistor and resonator are at the core of SiTime's new high performance oscillator platform. These MEMS-based oscillators are designed to achieve the performance requirements of high-end communication applications. The resonator, which has an f-Q product of 6.9×10^{12}, enables the oscillator to achieve sub- picosecond integrated phase jitter in the 12 kHz to 20 MHz frequency range. The MEMS thermistor, with a resistance-temperature sensitivity of 0.33 %/C, is used to compensate for the temperature-induced frequency variations of the silicon resonator. The thermistor is key to achieving sub-ppm frequency stability in a -40 C to 85 C temperature range and a sub-5 ppb Allan deviation in 0.1 second to 10 second strides. The demonstrated system performance opens high-volume data communication markets previously unavailable to MEMS-based oscillators.

INTRODUCTION

The multi-billion dollar timing market has motivated the development of MEMS resonator-based oscillators as a replacement for quartz crystal-based oscillators. MEMS-based oscillators leverage advantages common to semiconductor products, such as miniaturization and low-cost manufacturing. This is attractive for oscillators that are aimed at high-volume consumer and industrial applications. The requirements include tight specifications on phase noise, jitter, Allan deviation, long-term stability, temperature stability, and initial frequency tolerance. Successful product adoption requires meeting these performance requirements while creating a high-yielding, robust product with reduced cost and improved lead times.

Previously commercialized MEMS-based oscillators could not provide the system performance necessary to replace temperature-compensated quartz crystal oscillators (TCXOs) and ultra-low jitter oscillators used in a wide variety of telecommunication, networking, storage, wireless, and high speed serial protocol applications. Table 1 lists some of the typical performance requirements for these applications.

Table 1: Typical performance requirements for high-end data communication applications.

Specification	Requirements
Integrated phase jitter in 12 kHz-20 MHz offset from carrier	< 1 ps
Allan deviation in 0.1s-10s stride	< 5 ppb
Temperature Stability (-40 C to 85 C)	< 5 ppm
Initial Frequency Tolerance	< 1 ppm

We have recently demonstrated a new oscillator product platform that meets or exceeds the performance requirements described in Table 1 [1, 2]. In this paper, we focus on the role of MEMS in enabling these oscillators. We present an integrated 48 MHz silicon resonator and silicon thermistor that are at the core of SiTime's new oscillator product platform. The resonator exhibits a systematic ~3800 ppm frequency variation over a -40 C to 85 C temperature range, which is typical of uncompensated silicon
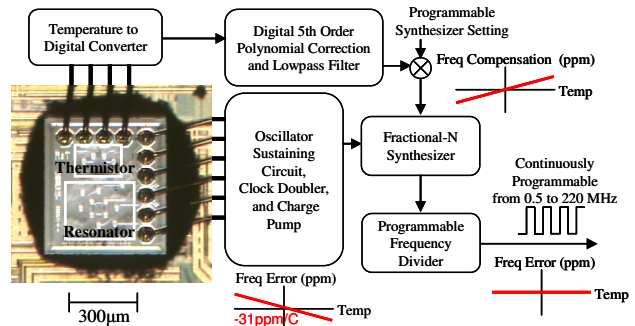

Figure 1: Block diagram of MEMS-based programmable oscillator. Micrograph shows assembled MEMS die stacked on CMOS die after dissolving plastic package. Both the resonator and thermistor are encapsulated in the MEMS die.

resonators. The output frequency of the oscillator is corrected to reduce temperature-induced variation in the resonator frequency. The compensation system uses the silicon thermistor, which is located on the same die as the resonator, and a high-resolution temperature-to-digital converter (TDC). The resulting oscillator achieves ±200 ppb frequency stability over a -40 C to 85 C temperature range. This high-performance oscillator product platform is accelerating the adoption of MEMS-based oscillators in the timing market.

SYSTEM OVERVIEW

Figure 1 shows a micrograph of the MEMS die stacked on top of the 0.18 μm CMOS die. The system architecture of the MEMS-based programmable oscillator achieves both temperature compensation and continuous frequency programmability. The MEMS resonator is combined with a sustaining circuit to create an electrical signal at the resonator's mechanical resonant frequency. However, due to the temperature sensitivity of the Young's Modulus of silicon, silicon resonators typically exhibit a frequency-temperature variation of -31 ppm/C [3].

A common approach to correct for the temperature-induced frequency change is to synthesize a temperature-corrected frequency using a TDC and polynomial correction logic. The TDC consists of a temperature sensitive element, to monitor the temperature of the MEMS die, and a converter to create a digital temperature value. A fractional-N phase-lock loop, in conjunction with a programmable frequency divider, is used to produce the desired temperature-stable output frequency of the oscillator.

A bipolar junction transistor (BJT) temperature sensor, which is integrated on the CMOS die, has previously been used as the temperature sensor. SiTime's new oscillator platform uses a silicon MEMS thermistor as the temperature sensitive element. This improves the measurement accuracy of the resonator's temperature and enables a TDC architecture which achieves 100 μK resolution in a 5Hz bandwidth [1].

The MEMS resonator and thermistor are co-fabricated on the same die using the SiTime MEMS First[TM] process [4]. Figure 2
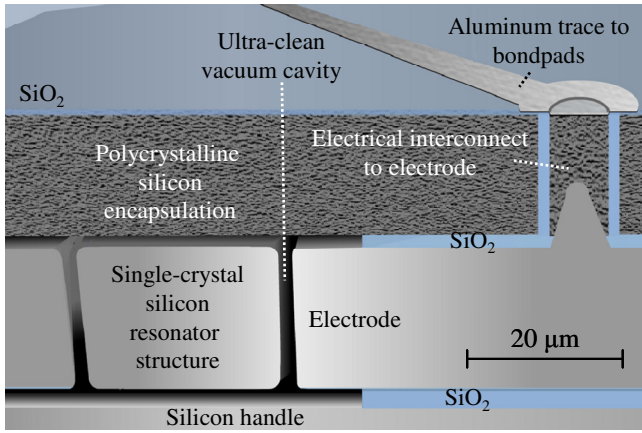
Figure 2: Cross-section diagram of SiTime's MEMS First^{TM} processes [4]. MEMS structures are wafer-level hermetically encapsulated using high-temperature epitaxial silicon.

shows a cross-section diagram of an encapsulated resonator. The MEMS structures are patterned in a silicon-on-insulator device layer. The cavity surrounding the structures is sealed during epitaxial deposition of the polycrystalline silicon encapsulation layer. This critical step provides a clean enclosure for the MEMS structures and protection from the external environment. The hermetic vacuum encapsulation of both devices is critical to achieving long-term frequency stability.

The packaged oscillators are produced using standard IC assembly practices. The MEMS and CMOS wafers are thinned to less than 150 μm using chemical mechanical polishing (CMP). Wafer-saw dicing and automated pick-and-place are used to assemble the die onto copper lead-frames. Wirebonds connect the resonator and thermistor to the sustaining circuit and TDC on the CMOS die, respectively. The encapsulation layer on the MEMS die is mechanically robust to plastic injection molding and subsequent package singulation. Standard IC processing allows the use of low-cost, high-volume plastic packaging in contrast to the expensive and specialized ceramic or metal packaging common to quartz resonators.

RESONATOR DESIGN

The 48 MHz resonator consists of four rings used for capacitive actuation and sensing (Figure 3). The four rings resonate in-phase in an extensional mode. The rings are coupled through frequency-matched crossed beams. A flexural-beam suspension connects the crossed beams to four mechanical anchors. The centrally-located anchors isolate the resonator from external mechanical stresses, such as those induced when the device is soldered to a circuit board. This stress isolation is an important factor in maintaining oscillator output frequency accuracy and initial frequency tolerance. Electrodes are placed on both the inside and outside of the rings for electrostatic transduction. The differential drive and sense configuration, shown in Figure 4, reduces capacitive feedthrough. High yield and tight frequency control (± 100 ppm) is achieved across a 200 mm wafer after CMP thinning (Figure 5).

The typical resonator quality factor, Q, of 144,000, is a result of a parallel combination of the Q due to various loss mechanisms [5]. High Q is critical in reducing both the far-from-carrier and close-to-carrier phase noise. Equation 1 is a simple model of phase noise, including the phase-noise floor, at a specified offset from carrier frequency [6]:
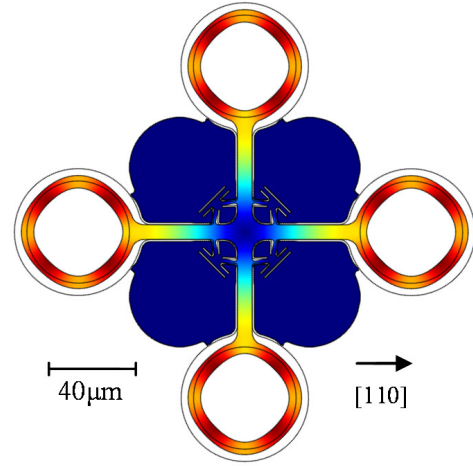

Figure 3: Finite element simulation of 48 MHz eigenmode of resonator. Exaggerated displacement shown.
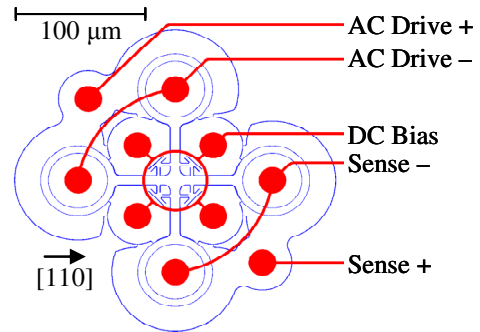

Figure 4: Drawing of silicon resonator and electrodes with metal interconnect routing in red
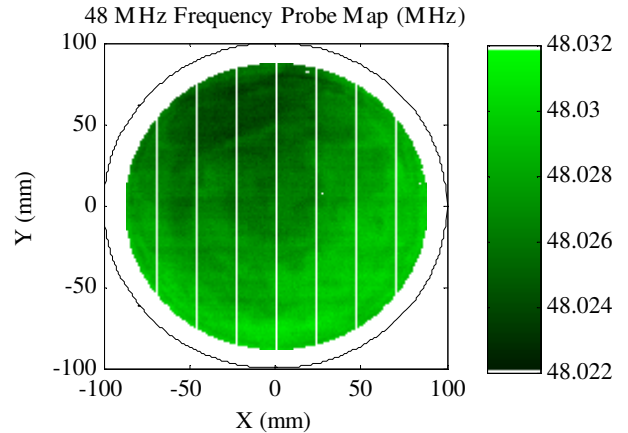

Figure 5: Resonant frequency map of 200 mm thinned wafer with ~70,000 48 MHz resonators showing frequency variation of ± 100 ppm across wafer.

$$L(\Delta\omega) = 10\log\left[\frac{2kT}{P_{sig}}\cdot\left(\frac{\omega_o}{2Q\Delta\omega}\right)^2 + 1\right] \quad (1)$$

where k is the Boltzmann's constant, T is absolute temperature in Kelvin, P_{sig} is the power output of the resonator, ω_o is the carrier frequency, Q is the quality factor, and $\Delta\omega$ is the frequency offset from the carrier frequency. Increasing Q helps to reduce the phase
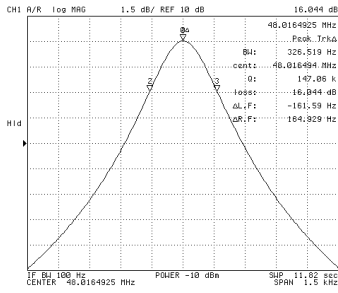
Figure 6: Network analyzer frequency response of MEMS 48 MHz resonator at 25 C.
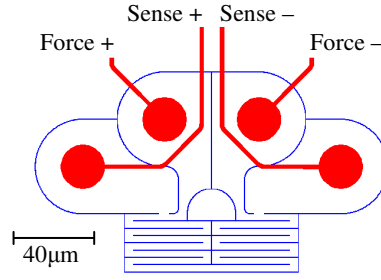

*Figure 7: Drawing of silicon thermistor configured for four-point measurement with metal routing in red.*

Figure 8: Temperature dependence of thermistor resistance and resonator frequency with 5th-order polynomial fit (lines) to data (points).

noise floor by reducing the motional resistance of the resonator and increasing its power output. At a given output power from the resonator, the close-to-carrier phase noise reduces with $1/Q^2$.

The resonator is designed to minimize the dominant energy loss mechanisms. Extensional vibration of the rings minimizes thermoelastic dissipation (TED). A Q_{TED} of 1.3×10^6 was determined for this resonator using a FEA method developed by Duwel, et al. [7]. Vacuum encapsulation of the resonator reduces gas-damping losses. At a cavity pressure of less than 1 Pa [8], the Q due to gas damping far exceeds 1×10^6 for this resonator. Optimization of the flexural suspension to reduce displacement at the anchor minimizes anchor losses. The Q due to the Akhieser effect is estimated to be 8.12×10^5 [9]. The f-Q product of the resonator, 6.9×10^{12}, is 5.6 times lower than the Akhieser limit of $\sim3.9\times10^{13}$ for silicon resonators. We believe that the Q of the resonator is limited by anchor loss mechanisms. However, the f-Q product achieved is comparable to some of the highest f-Q silicon resonators published (Figure 6) [9, 10].

THERMISTOR DESIGN

The silicon thermistor is a serpentine structure with four electrical contacts and four mechanical anchors (Figure 7). The thermistor is fabricated in the same single-crystal silicon device layer as the resonator. As such, the thermistor is hermetically vacuum encapsulated and anchored to isolate it from external mechanical stresses that adversely effect traditional BJT temperature sensors. Furthermore, the proximity of the thermistor to the resonator, less than 200 μm separation, improves thermal tracking of the temperature of the resonator compared to a temperature sensor integrated onto the CMOS die.

The four-point topology of the structure allows accurate measurement of the temperature-dependent resistance independent of the resistance of the wirebonds and metal interconnects. The temperature dependence of the conductivity of silicon, σ, can be calculated from the temperature-dependent carrier density and mobility of silicon using:

$$\sigma = q(n\mu_e + p\mu_h) \qquad (2)$$

where q is the electron charge, n is the density of electrons, μ_e is the electron mobility, p is the density of holes, and μ_h is the hole mobility. The carrier density and mobility in silicon have been empirically determined and are strong functions of both temperature and dopant concentration [11]. Both factors influence the sensitivity and linearity of the thermistor resistance.

Figure 8 shows the temperature dependence of the thermistor resistance and resonator frequency. With an overall resistance change of 40% from -40 C to 85 C, the MEMS thermistor-based TDC signal to noise ratio is an order of magnitude better than for a BJT-based TDC [1]. While the maximum thermistor sensitivity shown is ~0.33 %/C, the temperature dependence is not linear and
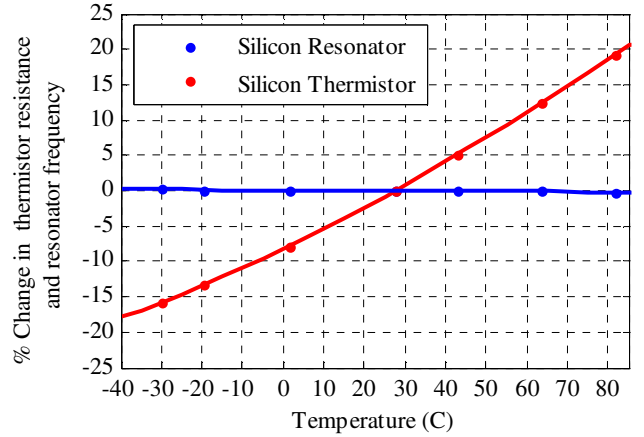
the thermistor sensitivity drops to 0.25 %/C at -40 C. Since both the resonator and resistor have higher order temperature dependencies, a 5th-order polynomial is used to correct the frequency of the resonator relative to the TDC output.

SYSTEM PERFORMANCE

Figure 9 shows the phase noise at 25 C of the combined 48 MHz resonator and sustaining circuit across extreme CMOS and MEMS manufacturing process corners. The 48 MHz resonator combined with the low-noise sustaining circuit dominates the oscillator phase noise floor between 10 kHz and 1 MHz. The phase noise of the 48 MHz resonator plus sustaining circuit is below -139 dBc/Hz at 10 kHz offset even at the most extreme CMOS and MEMS corner. The PLL bandwidth is set to 500 kHz to reduce noise contribution from other circuit blocks. The programmable oscillator achieves ~500 fs integrated phase jitter in the critical 12 kHz to 20 MHz range necessary for communication applications.

This thermistor-based TDC has been recently shown to achieve a state-of-art resolution of <100 μK in a 5 Hz bandwidth [1]. With a resolution of 100 μK, and a resonator sensitivity of -31 ppm/C, the Allan deviation has been demonstrated to be less than 5 ppb in 0.1 second to 10 second strides.

The frequency stability of the oscillator is shown in Figure 10. The frequency error of the compensated output is dominated by the fit quality of the polynomial used to correct the resonator frequency over a particular temperature range. The compensation achieves a ±200 ppb frequency stability in the industrial range of -40 C to 85 C. Implementation of higher order polynomial correction could further improve the frequency stability.
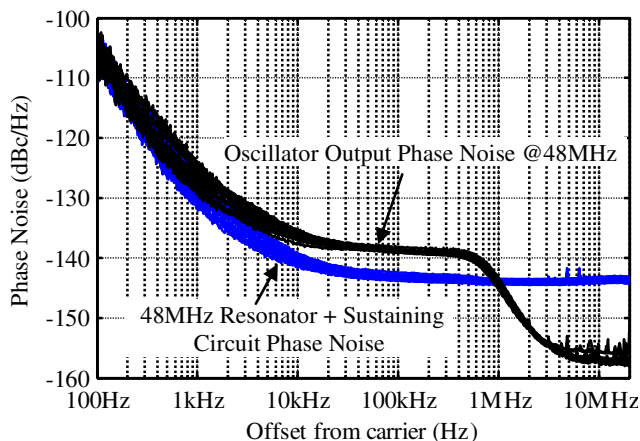
Figure 9: Phase noise at 25 C of 48 MHz MEMS plus sustaining circuit (blue) and compensated oscillator output (black). Nineteen devices are shown across extreme CMOS and MEMS process corners.
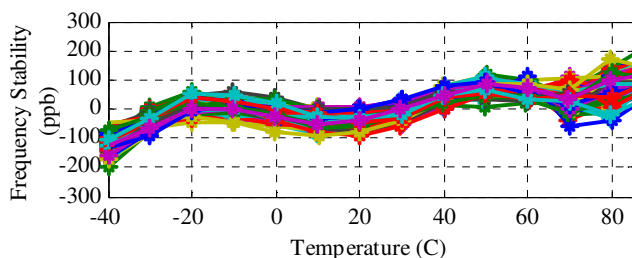

Figure 10: Frequency stability of oscillator output using 5th order polynomial compensation for 68 devices in -40 C to 85 C range.

CONCLUSION

The MEMS resonator and thermistor, described here, is instrumental in meeting the performance requirements for oscillators used in communication applications. The resonator provides the power-handling and high-Q necessary for low phase noise and low integrated phase-jitter oscillators. The thermistor is key to accurate temperature compensation of the silicon resonator. Both MEMS structures are fabricated in SiTime's MEMS First[TM] process that provides a robust wafer-level hermetic encapsulation for long-term stability and compatibility with standard IC packaging processes.

ACKNOWLDEGEMENTS

Michael Perrott, Jim Salvia, Fred Lee, Shouvik Mukherjee, Jin-Tae Kim, Sassan Tabatabaei, Sudhakar Pamarti, Bruno Garlepp, Cathy Lee, and Haechang Lee developed the CMOS architecture.

REFERENCES

[1]   M. Perrott, J. Salvia, F. Lee, A. Partridge, S. Mukherjee, C. Arft, J-T. Kim, N. Arumugam, P. Gupta, S. Tabatabaei, S. Pamarti, H. Lee, F. Assaderaghi. "A Temperature-to-Digital Converter for a MEMS-based Programmable Oscillator With Better than ±0.5 ppm Frequency Stability". IEEE International Solid-State Circuits Conference, 19-23 Feb. 2012

[2]   F.S. Lee, J. Salvia, C. Lee, S. Mukherjee, R. Melamud, N. Arumugam, S. Pamarti, C. Arft, P. Gupta, S. Tabatabaei, B. Garlepp, H. Lee, A. Partridge, M.H. Perrott, and F. Assaderaghi, F, "A programmable MEMS-based clock generator with sub-ps jitter performance," Symposium on VLSI Circuits (VLSIC), pp.158-159, 15-17 June 2011

[3]   C. Bourgeois, E. Steinsland, N. Blanc, and N.F. de Rooij , "Design of resonators for the determination of the temperature coefficients of elastic constants of monocrystalline silicon," Proceedings of the 1997 IEEE International Frequency Control Symposium, pp.791-799, 28-30 May 1997

[4]   SiTime Corporation, "SiTime's MEMS First[TM] Process," http://www.sitime.com/support/application-notes

[5]   M. Weinberg, R. Candler, S. Chandorkar, J. Varsanik, T.W. Kenny, and A. Duwel, "Energy loss in MEMS resonators and the impact on inertial and RF devices," Solid-State Sensors, Actuators and Microsystems Conference, TRANSDUCERS 2009. pp.688-695, 21-25 June 2009

[6]   Lee T.H., The Design of CMOS Radio-Frequency Integrated Circuits, 2nd Edition, Cambridge University Press, New York, 2004.

[7]   A. Duwel, R.N. Candler, T.W. Kenny, and M. Varghese, "Engineering MEMS Resonators With Low Thermoelastic Damping," Journal of Microelectromechanical Systems, vol.15, no.6, pp.1437-1445, Dec. 2006.

[8]   R.N. Candler, M.A. Hopcroft, B. Kim, W.-T. Park, R. Melamud, M. Agarwal, G. Yama, A. Partridge, M. Lutz, and T.W. Kenny, "Long-Term and Accelerated Life Testing of a Novel Single-Wafer Vacuum Encapsulation for MEMS Resonators," Journal of Microelectromechanical Systems, vol.15, no.6, pp.1446-1456, Dec. 2006

[9]   S.A. Chandorkar, M. Agarwal, R. Melamud, R.N. Candler, K.E. Goodson, and T.W. Kenny, "Limits of quality factor in bulk-mode micromechanical resonators," IEEE International Conference on Micro Electro Mechanical Systems, MEMS 2008. pp.74-77, 13-17 Jan. 2008

[10] J.T.M van Beek and R. Puers, "A review of MEMS oscillators for frequency reference and timing applications", Journal of Micromech. Microeng. 22 (2012)

[11] S.M. Sze, Physics of Semiconductor Devices, 2nd Edition, John Wiley & Sons, New York, 1981

CONTACT

R. Melamud, rmelamud@gmail. com